Improved Far-Field Angle in Narrow-Ridge High-Power Laser Diodes Using a Double Stripe Structure

Daehong Kim, Jung-Tack Yang, Woo-Young Choi, *Member, IEEE*, and Younghyun Kim, *Member, IEEE*

***Abstract*—We propose a novel double stripe structure for achieving a narrow far-field angle without significant output power loss in narrow-ridge high-power broad-area laser diodes. By introducing double SiO_2 stripes on the top side of the laser diode, we effectively suppress high-order modes through mode weight engineering. Through self-consistent electro-thermal-optical simulations powered by LASTIP with the well-verified model from the reference, we comprehensively analyze and compare the characteristics of high-power broad-area laser diodes utilizing the loss tailoring technique that adopted the much simpler structure compared to prior study and our proposed structure. Our results demonstrate a significant reduction of approximately 36% in the far-field angle while maintaining slope efficiency. This approach shows promise for enhancing the performance of coupling efficiency between narrow-ridge high-power laser diodes and fibers.**

***Index Terms*—Far-field angle, high-power laser diode, lateral modes, loss tailoring, mode weight engineering.**

I. Introduction

HIGH-POWER laser diodes (HPLDs) are widely used as the pumping source for many types of high-power lasers for various applications such as military, industrial, and consumer usage. It has its advantages in high electrical efficiency, low cost, and small size [1], [2], [3]. However, their performances suffer from self-heating, which causes the thermal rollover resulting in limited maximum output power and far-field (FF) blooming causing reduced pump beam coupling efficiency [4]. Therefore, narrowing the FF angle while sustaining high power efficiency is a major challenge for high-power laser diodes as pumping sources.

Manuscript received 4 August 2023; revised 12 October 2023; accepted 3 November 2023. Date of publication 8 November 2023; date of current version 22 November 2023. This work was supported in part by the Technology Innovation Program (20015909) through the Korea Evaluation Institute of Industrial Technology (KEIT), funded by the Ministry of Trade, Industry & Energy (MOTIE, Korea), and in part by Korea Basic Science Institute (National research Facilities and Equipment Center) grant funded by the Ministry of Education (grant No. 2023R1A6C103A035, No. 2021R1A6C101A405). *(Corresponding author: Younghyun Kim.)*

Daehong Kim and Younghyun Kim are with the Department of Photonics and Nanoelectronics, BK 21 FOUR ERICA-ACE Center, Hanyang University, Ansan 15588, South Korea (e-mail: altair45@hanyang.ac.kr; younghyunkim@hanyang.ac.kr).

Jung-Tack Yang and Woo-Young Choi are with the Department of Electrical and Electronic Engineering, Yonsei University, Seoul 120-749, South Korea (e-mail: zerg0522@gmail.com; wchoi@yonsei.ac.kr).

Digital Object Identifier 10.1109/JPHOT.2023.3331194

HPLDs have usually a wide emitter size and easily lead to multiple lateral modes [5]. For specific laser diode chips, a thermal lens induced by self-heating and lateral carrier accumulation at the stripe edges plays the most critical role, leading to a rising number of lateral modes at high-power operation. At high currents, the increased lateral temperature gradient in HPLDs leads to a rise in the lateral index step, detrimentally attributing to the propagation of higher-order modes. Consequently, HPLDs often exhibit a widening of the lateral FF angle as the current increases [6]. To address this issue, various methods have been proposed to reduce the number of lateral modes and FF angles, which have demonstrated promising results through experiments or simulations. Such as pedestal heat sink structure to reduce thermal lens effect [7], [8]. Reducing the width of the emitter to decrease the number of modes [9], and a consistent gain profile throughout the contact region is advantageous for enhancing optical field stabilization by employing structures that tailor the gain or optimize the current path. Examples of such structures include the phase-locked array, multi-stripe gain structure, or current modulation structure [10], [11], [12]. The effective enhancement of beam quality can be achieved through the successful mitigation of lateral carrier accumulation via deep proton implantation [13]. Introducing mode filters is another effective approach for inducing additional losses specifically targeting high-order modes. Examples of such mode filters include tapered lasers, phase structures, external cavity configurations, tilted waveguides, microstructures, and inhomogeneous waveguides [14], [15], [16], [17], [18], [19], [20], [21]. However, these methods are subject to limitations, as they often come at the cost of decreased output power or require complex designs, which restrict their practical applicability.

According to a recent study, they reported the successful achievement of a substantial decrease in the FF angle without incurring significant power losses by employing loss tailoring using micro-scale triangular holes [6]. The structure of the loss tailoring structure laser diode from the prior study is explained in Fig. 1(f). To mitigate the presence of high-order lateral modes, triangular-shaped micro-holes are strategically positioned along the optical peak locations of these high-order modes. However, this method is not suitable for narrow-ridge laser diodes (LDs) designed for short wavelengths, primarily due to the size limitations of the holes and the complexity of placement. The previous study employed an LD model with a ridge width of

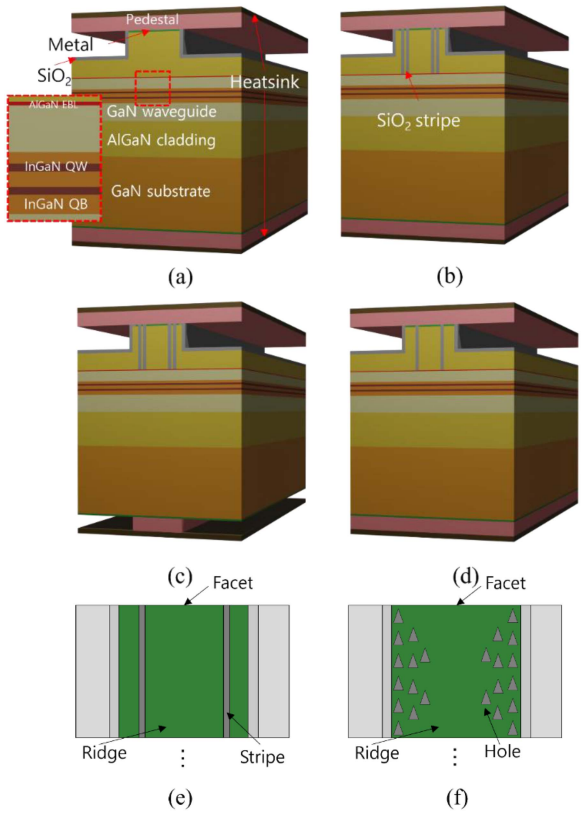

Fig. 1. (a) Original, (b) loss tailoring model with simple stripe, (c) simple stripe with short double pedestal structure, and (d) double stripe model, top view of (e) double stripe model, and (f) loss tailoring structure from [6] respectively.

100 μm with 5 μm-width triangular holes for loss tailoring. In contrast, the short-wavelength HPLDs reported so far tend to have narrower ridges, less than 30 μm [22], [23], [24]. Adopting the 5 μm-width holes in these LDs would considerably decrease the contact area and may also suppress lower-order modes. As a result, the overall performance of the LDs would be degraded. Additionally, in the case of narrow-ridge laser diodes, the arrangement of the holes in such models will be more crowded and closely spaced compared to the previous model. This increased density of the holes poses a challenge in terms of fabrication, requiring a more accurate and precise process. Consequently, the manufacturing process for the short-wavelength model is expected to incur additional time and cost due to the heightened complexity and precision demands.

In this paper, we propose a new structure based on a loss tailoring structure using simple stripes (SSLT), which is based on a similar mechanism to the aforementioned research. Unlike prior research, we implemented stripes instead of triangular holes for reasonable adaption to short-ridge laser diode and simplification of fabrication as described in Fig. 1(e). Also, we introduce two additional improved structures derived from all SSLT models. We investigate and compare the characteristics of lateral mode profiles from the proposed structures through numerical simulations.

II. Simulation Method and its Verification

For the numerical analysis of high-power laser diodes, we utilize the commercially available simulator LASTIP [25]. It enables self-consistent simulations of the electrothermal-optical properties of laser diodes, including essential aspects such as electron and hole transport, quantum well optical gain, and heat dissipation in the transverse plane. In our simulations, we account for various heat sources, including Joule heating and heat generated from optical modal absorption and non-radiative recombination processes. By incorporating these comprehensive thermal and optical considerations, we can accurately model and analyze the performance characteristics of high-power laser diodes. We have studied improving high-power laser diodes in terms of beam quality or decreasing FF by using the same verified simulation method. Details also can be found in our previous works [8], [26], [27], [28], [29]. To verify its accuracy, we first simulate a high-power laser diode chip and mount that structure as described in a published paper [22], [30].

The layer structure of the laser diode and its mount structure is shown in Fig. 1(a). The 405-nm laser diode has a 12-μm-wide rib and 1200-μm-long cavity with facet reflectivities of 5.6% and 95.0%. It consists of $In_{0.066}GaN$ multiple quantum wells and $In_{0.008}GaN$ quantum barriers with thick GaN upper and lower waveguides. Between the p-side waveguide and cladding layer, there is a highly p-doped $Al_{0.36}GaN$ 5-nm-thick electron blocking layer to increase efficiency.

The mount consists of AlN upper and SiC lower sub-mount, both are connected and only the lower one is directly connected to the package and thermoelectric cooler (TEC). The temperatures at the very top metal above the rib waveguide and the very bottom metal below the 80-μm-thick GaN substrate are assumed to remain at the heat sink temperatures of 298 K. It is important to consider the thermal index change for separate confinement heterostructure (SCH) layers because it is the main cause for the FF blooming. For this, we use 1.3×10^{-4} / K as the temperature dependence of the thermal index change for GaN [31]. Additionally, the influence of free-carrier absorption and carrier-induced refractive index change is taken into account in our analysis. Subsequently, the transversal lasing modes are calculated in a self-consistent manner by considering the perturbed refractive index profile derived from the Helmholtz equation. This comprehensive approach allows us to accurately assess and characterize the behavior of the lasing modes in our study.

We first carried out model verification using the laser diode structure in Fig. 1(a), which is reported in the reference [32]. Fig. 2(a) presents vertical profiles depicting the refractive index and the simulated lasing mode. Fig. 2(b) displays the simulated light power, current, and voltage characteristics alongside the reference data for the laser diode structure as described in Fig. 1(a). To reproduce the experimental results shown in Fig. 2, we used the Auger coefficient of $C_n = 6.5 \times 10^{-30}$ cm^6/s and $C_p = 6 \times 10^{-31}$ cm^6/s at room temperature, adopted absorption cross-section of 0.6×10^{-18} cm^2 and modal loss of 2/cm at $T = \Delta 110$K as a fitting parameter. As shown in Fig. 2, all simulated results agree well with the reference data, indicating well-verified model and simulation setups.

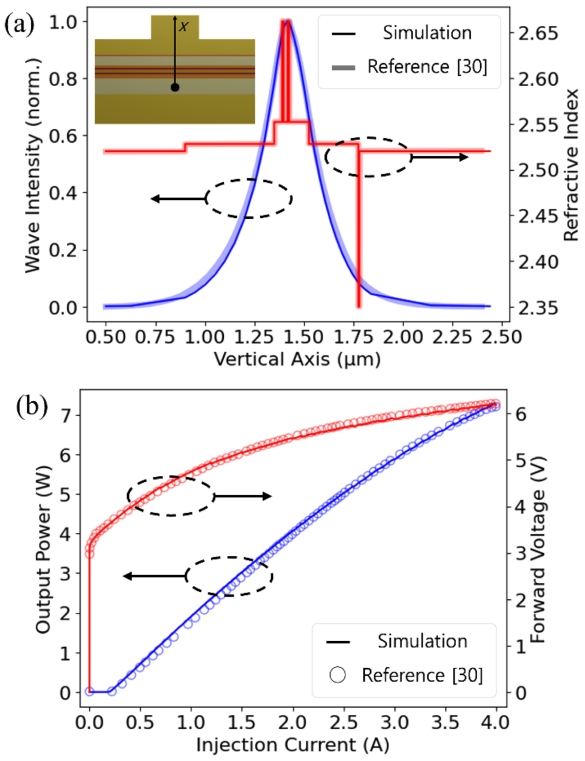

Fig. 2. (a) Vertical profiles of the refractive index and lasing mode (b) L-I-V characteristic of simulated model and reference.

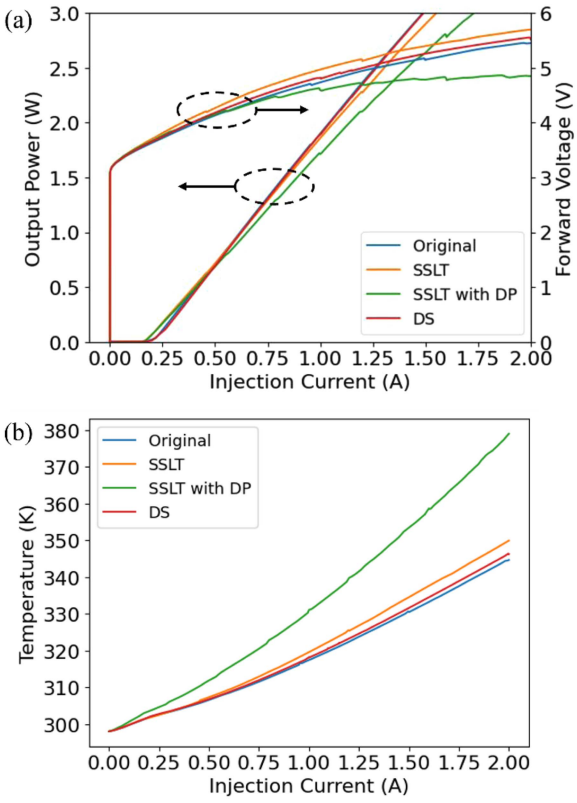

Fig. 3. (a) L-I-V characteristic and (b) max temperature comparison of all models.

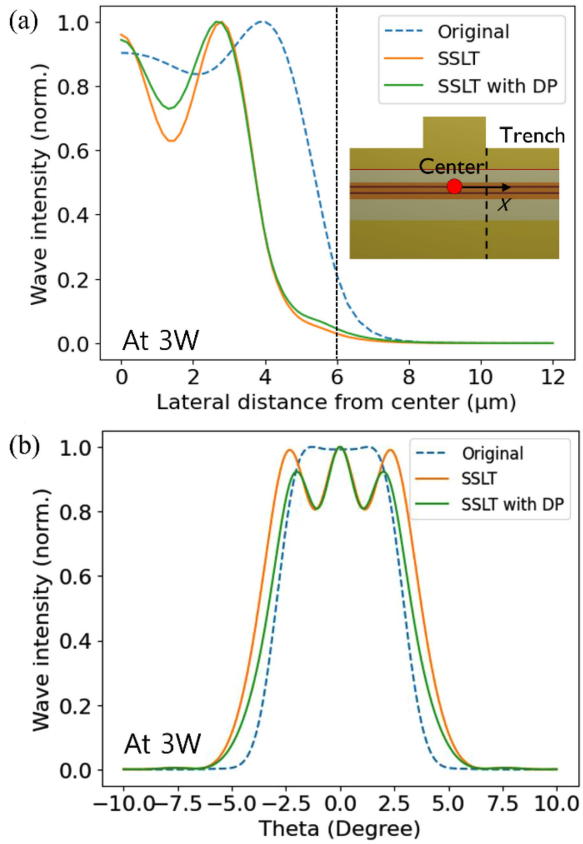

Fig. 4. (a) Near-field and (b) far-field pattern angle comparison of the original and all loss tailoring models at an optical power of 3W. The red dot and dotted line of the inset in (a) indicate the center and the border between the trench and rib respectively.

III. Performance Comparison of Laser Diodes With and Without Simple Stripe Loss Tailoring

In this section, we present a comparison of laser diode performance between the original design and the SSLT, as illustrated in Fig. 1(a) and (b), respectively. In a previous study, 5-μm-wide triangular holes were used to make additional losses for high-order modes. Instead of using small triangles, we propose a simpler rectangular stripe structure. This structure consists of a total of 4 stripes, each with a width of 0.5 μm, filled with SiO_2, and positioned at the peak points of the high-order modes.

To facilitate a comprehensive comparison of the LD performances, we conducted electro-optical simulations considering internal temperature for the original model (Fig. 1(a)), the model based on the loss tailoring technique (Fig. 2(b) and (c)), and the newly proposed model (Fig. 1(d)). Fig. 3(a) and (b) present the light output power, current, and voltage (L-I-V) characteristics and the maximum temperature of the laser diode (LD). The original model exhibits the best light power and current (L-I) performance among all the models, achieving a power output of 3 W at a current of 1.5 A. The double stripe (DS) model demonstrates nearly identical slope efficiency compared to the original, with only a slight reduction in the I-V performance. This reduction can be attributed to the decrease in the p-contact

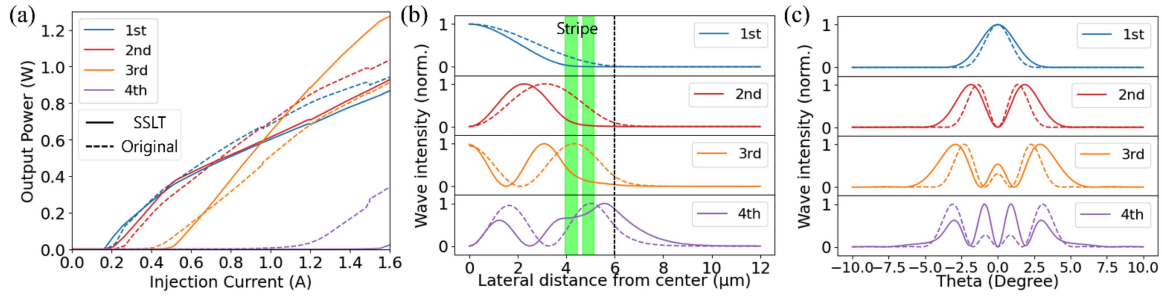

Fig. 5. (a) Mode power intensity, (b) near-field mode intensity, and (c) far-field mode intensity comparison of the loss tailoring with simple stripe model at 3W.

area caused by the presence of the stripe. The SSLT model achieves 3 W at a current of 1.55 A, while the SSLT with double pedestals (DP) achieves the same power output but at a higher current of 1.75 A. The maximum temperature follows the trend: SSLT with DP > SSLT > DS > original models, correlating with the inverse relationship between temperature and contact area. Higher temperatures explain the degraded performance of the L-I characteristic. In the case of current and voltage performance, previous studies on GaN-based laser diodes show that self-heating caused by the high activation energy of Mg dopant reduces series resistance [33]. In SSLT and DS structures, reduced contact area and slight temperature increase raise operating voltage. However, in SSLT with DP, the significant temperature increase activates holes, compensating for the voltage increase from a minimal contact area.

To compare the slow axis angle of all models, we simulated near-field (NF) and far-field (FF) patterns. Fig. 4(a) and (b) illustrate the NF and FF characteristics of the original, SSLT, and SSLT with DP, respectively. In Fig. 4(a), it can be observed that the SSLT model achieved a narrower NF compared to the original model. However, Fig. 4(b) indicates a larger FF for the SSLT model. In particular, the FF angle increased from 5.8° to 7.4° for the full width at half-maximum (FWHM) and from 8.4° to 10.8° for the 95% power inclusion ($\theta_{// 95\%}$). Fig. 5(a) presents a comparison of the power distribution among all the modes in both the SSLT and original models. It is evident that the highest-order mode (the 4th-order mode in this case) is suppressed, while the 3rd-order mode is significantly stronger compared to the original model due to mode competition. Fig. 5(b) shows the lateral NF modes for both models. The green columns show where the stripes are, and they are located on the peak of 3rd and 4th-order modes. The result reveals a shrinkage of all modes except the 4th mode, which explains the narrower NF observed in the SSLT model.

Fig. 5(c) presents the FF patterns for the 4 modes corresponding to each NF pattern in the laser diodes. Each mode is normalized to its own mode. Despite the negligible power of the highest-order mode, the powerful 3rd-order mode, and the narrow NF result in a wider FF for the SSLT's 3rd-order mode compared to the 4th-order mode of the original model.

The thermal lens effect is one of the main reasons that can cause wider FF. The non-uniform temperature profile inside the waveguide leads to different lateral refractive index profile that enhances the index guiding of laser modes [34]. To mitigate its effect, there was a study that adopted a pedestal to reduce the non-uniform index profile [7]. So, we simulated the lateral refractive index profile of the SSLT model and compared it to the original model in Fig. 6 to whether we can suppress the highest order mode of the SSLT model. The figure depicts that the SSLT model exhibits a greater difference in refractive index between the center and edge regions. Therefore, we incorporate a double pedestal structure based on a prior study that demonstrated an improved index difference and FF angle [8]. The SSLT with double pedestal model (SSLT with DP) shares the same layer structure as the SSLT model, but it features a narrower width for the bottom contact pedestal (12 μm), as illustrated in Fig. 1(c). Consequently, the index difference is significantly reduced, as shown in Fig. 6. However, due to the reduced contact area

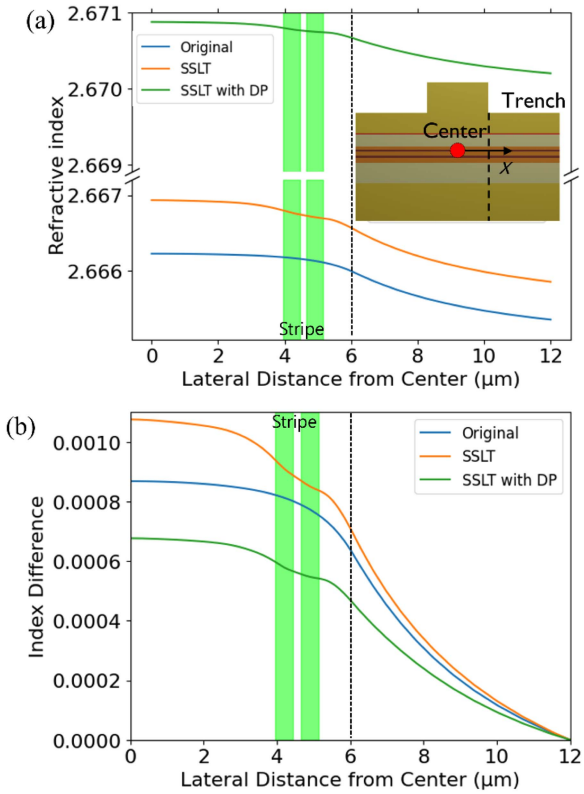

Fig. 6. (a) Refractive index and (b) index difference from refractive index of 12 μm point at the optical output power of 3 W.

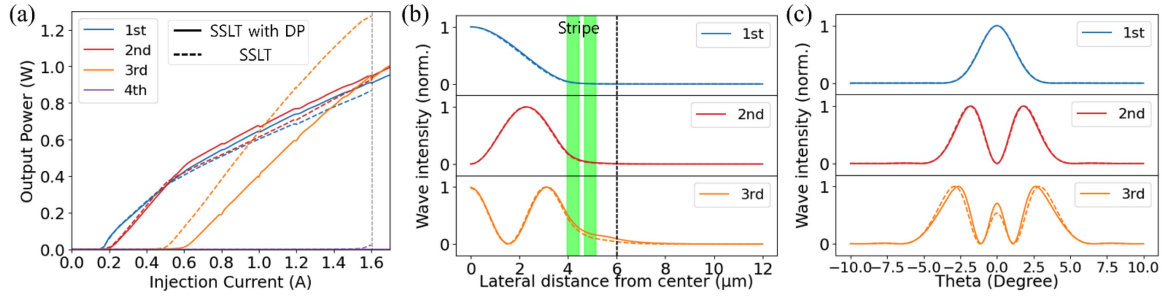

Fig. 7. (a) Mode power intensity, (b) near-field mode intensity, and (c) far-field mode intensity comparison of the loss tailoring with simple stripe and the double pedestal model at 3W.

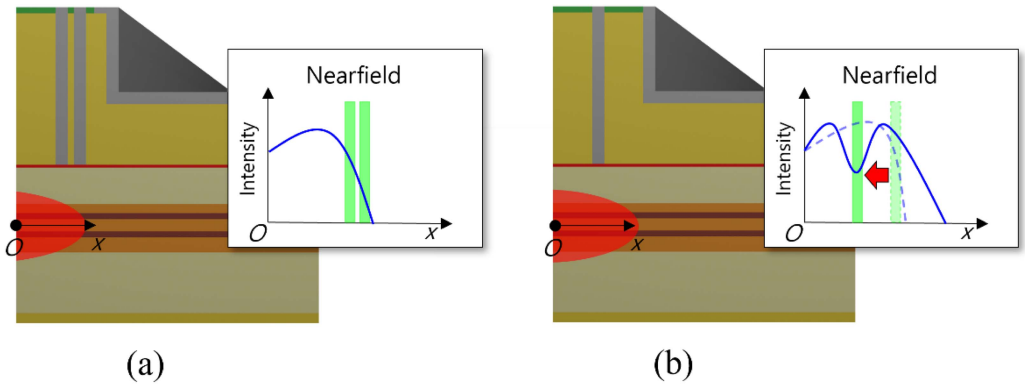

Fig. 8. Mode and near-field of (a) the loss tailoring with simple stripe and (b) the double stripe model.

and cooling efficiency, the maximum temperature experiences a drastic increase, leading to a severe degradation of slope efficiency, as observed in Fig. 3.

While the lateral distance from the center of the NF pattern remains almost identical to the SSLT model, the FF angle of the SSLT with DP model decreases from 7.4° to 6.5° for the FWHM, with a negligible change for $\theta_{//\ 95\%}$. To comprehensively analyze the results, a detailed comparison was conducted between the SSLT and the SSLT with DP models, as shown in Fig. 7. Fig. 7(a) presents a comparison of the mode powers between the SSLT and SSLT with DP models. Fig. 7(b) focuses on the comparison of the lateral NF modes. Lastly, Fig. 7(c) provides a comparison of the FF patterns of all the modes. The results in Fig. 7(a) indicate that the DP structure primarily affects the rise of the 3rd-order mode while strengthening the 1st and 2nd-order modes, with minimal influence on the NF and FF patterns shown in Fig. 7(b) and (c). The SSLT with DP approach may effectively weaken the highest-order mode (The 3rd-order mode in this case), but it fails to completely suppress it. Additionally, its FF angle remains wider than the original model due to the narrow NF pattern coupled with poor slope efficiency.

IV. Proposal of Double Stripe Model for Mode Weight Engineering

We introduce the DS structure (Fig. 1(d)) for mode weight engineering as a method to improve the FF angle of laser diodes while maintaining laser efficiency and output power. To provide a comprehensive understanding of the DS model, we present Fig. 8. Fig. 8(a) shows the SSLT structure, specifically designed to introduce losses to high-order modes. In contrast, Fig. 8(b) indicates the DS structure, which aims to shift a lower-order mode towards the edge while simultaneously suppressing the high-order mode. The DS structure offers a promising approach to achieve an improved FF angle without compromising laser efficiency and power.

To validate the effectiveness of our proposed technique, simulations and analyses were performed on the DS structure and compared with the original structure. Fig. 9(a) illustrates the comparison of mode power between the DS structure and the original model. For the original model, as the current increased, the modes gradually generated from the 1st to the 4th mode. However, for the DS model, the 2nd-order mode keeps rising as a dominant optical mode suppressing the generation of the 3rd and 4th-order modes. Fig. 9(b) shows the NF pattern of the DS model, indicating that the shift of the 2nd-order mode causes the mode to overlap completely with the peak of the 3rd-order mode and it results in suppressing the 3rd mode. In Fig. 9(c), we demonstrate how the shift of the NF pattern affects the FF pattern. Based on Fig. 9(b), the shift of the 2nd-order mode toward the edge caused widened NF. As a result, a narrower FF of the 2nd-order mode is observed in Fig. 9(c).

We compared all NF patterns and FF pattern angles in Fig. 10. In Fig. 10(a), we present a comprehensive comparison of all the

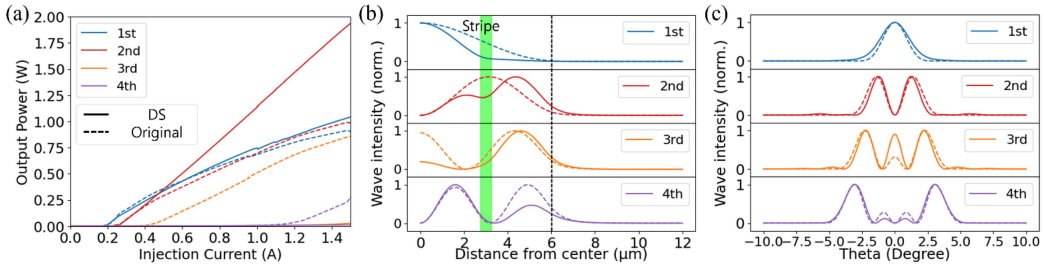

Fig. 9. (a) Mode power intensity (b) near-field mode intensity and (c) far-field mode intensity comparison of the double stripe model at 3W.

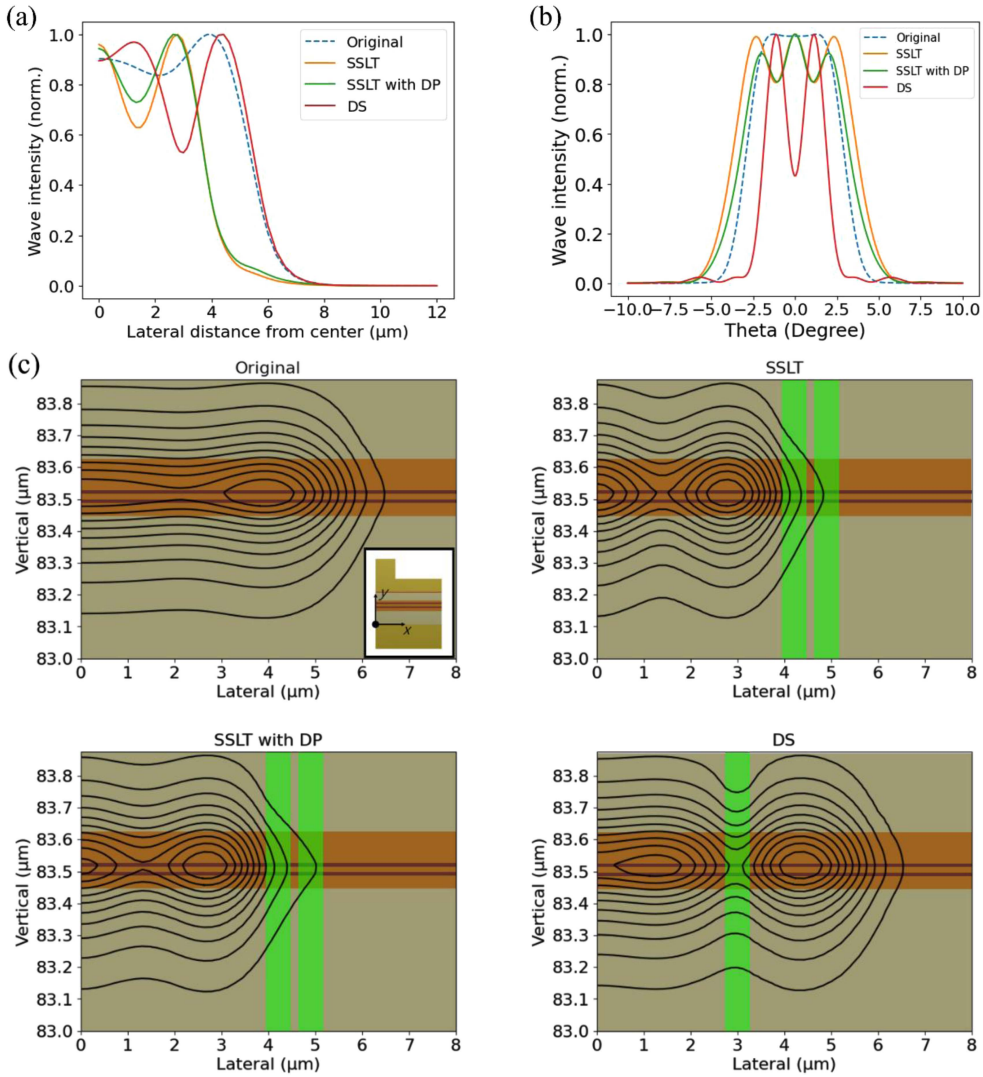

Fig. 10. (a) Near-field and (b) far-field angle, and (c) 2D near-field comparison of the original, all loss tailoring models, and the double stripe model at an optical power of 3W.

models introduced in this paper and the data proved that the DS model achieved the widest NF of all. But it has a nearly identical width compared to the original. However, Fig. 10(b) shows that the DS model achieves the narrowest slow axis angle of 3.8° and 5.4° for the FWHM and $\theta_{//\ 95\%}$, respectively, representing a 36% reduction compared to the original model, which has an FF angle of 5.8° and 8.4° in the same manner. This is because the DS model has fewer modes compared to the original as mentioned above in Fig. 9(a). Consequently, the stripe shifts the 2nd-order mode to the edge as shown in Fig. 8(b), causing the suppression of the high-order mode generation. Therefore, it dominates the optical power. Also, the NF of the 2nd-order mode is as wide as that of the 3rd-order mode, resulting in a narrower FF angle.

The reference achieved better results, approximately a 50% decrease, compared to our work [6]. However, the results showed that the loss tailoring method is not effective for the short-ridge

structures. Instead of causing selective loss to high-order modes, the DS model achieved such results by decreasing lateral modes from 5 to 2. Furthermore, the DS model widened the 2nd-order mode by implementing the stripe and maintained the identical NF width compared to the original model. Thus, the DS model proved its worth for short-wavelength laser diodes.

V. Conclusion

We have introduced a novel design for a narrow-ridge high-power broad-area laser diode incorporating stripes, which effectively suppress high-order modes and broaden the lateral NF pattern. By the new model, we achieved a 36% reduced FF angle with negligible slope efficiency decrease. Through numerical simulations, we have successfully demonstrated that the proposed DS structure can achieve a narrower lateral FF angle without a significant decrease in slope efficiency, in contrast to the previously reported loss tailoring technique. Additionally, this study, conducted using a simulation method validated with experimental data, is anticipated to yield similar results in future experiments. Moreover, the simplification of essential procedural steps in the implementation is deemed advantageous for empirical validation. Therefore, the proposed structure in this study holds promise for enhancing beam quality.

References

[1] A. V. Aluev, A. M. Morozyuk, M. S. Kobyakova, and A. A. Chel'nyi, "High-power 2.5-W cw AlGaAs/GaAs laser diodes," *Quantum Electron.*, vol. 31, no. 7, pp. 627–628, Jul. 2001, doi: 10.1070/QE2001v031n07ABEH002016.

[2] V. Gapontsev et al., "Highly-efficient high-power pumps for fiber lasers," *Proc. SPIE*, vol. 10086, pp. 16–25, 2017, doi: 10.1117/12.2250634.

[3] L. Zhong and X. Ma, *Optoelectronics: Devices and Applications*. London, U.K.: Intechopen, 2011.

[4] P. Crump, S. Böldicke, C. M. Schultz, H. Ekhteraei, H. Wenzel, and G. Erbert, "Experimental and theoretical analysis of the dominant lateral waveguiding mechanism in 975 nm high power broad area diode lasers," *Semicond. Sci. Technol.*, vol. 27, no. 4, Feb. 2012, Art. no. 045001, doi: 10.1088/0268-1242/27/4/045001.

[5] S. Gross, D. W. Coutts, M. Dubinskiy, and M. J. Withford, "Beam shaping of a broad-area laser diode using 3D integrated optics," *Opt. Lett.*, vol. 44, no. 4, pp. 831–834, Feb. 2019, doi: 10.1364/OL.44.000831.

[6] L. Wang et al., "Loss tailoring of high-power broad-area diode lasers," *Opt. Lett.*, vol. 44, no. 14, pp. 3562–3565, Jul. 2019, doi: 10.1364/OL.44.003562.

[7] J. Piprek, "Inverse thermal lens effects on the far-field blooming of broad area laser diodes," *IEEE Photon. Technol. Lett.*, vol. 25, no. 10, pp. 958–960, May 2013, doi: 10.1109/lpt.2013.2255590.

[8] Y. Kim, J.-T. Yang, and W.-Y. Choi, "High-power broad-area laser diode performance improvement with a double pedestal structure," *Jpn. J. Appl. Phys.*, vol. 58, no. 4, Apr. 2019, Art. no. 042004, doi: 10.7567/1347-4065/ab0c71.

[9] Y. Li et al., "High brightness narrow-stripe broad-area diode lasers at 976 nm," *Proc. SPIE*, vol. 11023, pp. 1121–1125, 2019, doi: 10.1117/12.2521923.

[10] W. Zhou, S. Slivken, and M. Razeghi, "Phase-locked, high power, mid-infrared quantum cascade laser arrays," *Appl. Phys. Lett.*, vol. 112, no. 18, Apr. 2018, Art. no. 181106, doi: 10.1063/1.5028281.

[11] G. S. Maląg, E. Dąbrowska, and M. Teodorczyk, "Emitted beam stabilization in junction plane by lateral periodic structure in laser diodes emitting at 980 nm," *Proc. SPIE*, vol. 10974, pp. 27–34, 2018, doi: 10.1117/12.2516448.

[12] T. Wang et al., "Injection-insensitive lateral divergence in broad-area diode lasers achieved by spatial current modulation," *Appl. Phys. Exp.*, vol. 9, no. 11, Oct. 2016, Art. no. 112102, doi: 10.7567/apex.9.112102.

[13] M. Winterfeldt, P. Crump, S. Knigge, A. Maaßdorf, U. Zeimer, and G. Erbert, "High beam quality in broad area lasers via suppression of lateral carrier accumulation," *IEEE Photon. Technol. Lett.*, vol. 27, no. 17, pp. 1809–1812, Sep. 2015, doi: 10.1109/LPT.2015.2443186.

[14] L. Wang et al., "Near-diffraction-limited Bragg reflection waveguide lasers," *Appl. Opt.*, vol. 57, no. 34, pp. F15–F21, Dec. 2018, doi: 10.1364/AO.57.000F15.

[15] H. C. Eckstein, U. D. Zeitner, A. Tunnermann, W. Schmid, U. Strauss, and C. Lauer, "Mode shaping in semiconductor broad area lasers by monolithically integrated phase structures," *Opt. Lett.*, vol. 38, no. 21, pp. 4480–4482, Nov. 2013, doi: 10.1364/OL.38.004480.

[16] S. Hengesbach, S. Klein, M. Traub, and U. Witte, "Simultaneous frequency stabilization, wavelength multiplexing and improvement of beam quality using a self-optimizing external cavity diode laser," *Opt. Lett.*, vol. 41, no. 3, pp. 595–598, Jan. 2016, doi: 10.1364/OL.41.000595.

[17] Y. Zhao et al., "Going beyond the beam quality limit of spectral beam combining of diode lasers in a V-shaped external cavity," *Opt. Exp.*, vol. 26, no. 11, pp. 14058–14065, May 2018, doi: 10.1364/OE.26.014058.

[18] D. Heydari, Y. Bai, N. Bandyopadhyay, S. Slivken, and M. Razeghi, "High brightness angled cavity quantum cascade lasers," *Appl. Phys. Lett.*, vol. 106, no. 9, Mar. 2015, Art. no. 091105, doi: 10.1063/1.4914477.

[19] J. Rong et al., "Low lateral divergence 2 μm InGaSb/AlGaAsSb broad-area quantum well lasers," *Opt. Exp.*, vol. 24, no. 7, pp. 7246–7252, Mar. 2016, doi: 10.1364/OE.24.007246.

[20] R. Kaspi, S. Luong, C. Yang, C. Lu, T. Newell, and T. Bate, "Extracting fundamental transverse mode operation in broad area quantum cascade lasers," *Appl. Phys. Lett.*, vol. 109, no. 21, Nov. 2016, Art. no. 211102, doi: 10.1063/1.4968800.

[21] M. J. Miah, S. Strohmaier, G. Urban, and D. Bimberg, "Beam quality improvement of high-power semiconductor lasers using laterally inhomogeneous waveguides," *Appl. Phys. Lett.*, vol. 113, no. 22, Nov. 2018, Art. no. 221107, doi: 10.1063/1.5054645.

[22] M. Kawaguchi et al., "Optical-loss suppressed InGaN laser diodes using undoped thick waveguide structure," *Proc. SPIE*, vol. 9748, pp. 99–108, 2016, doi: 10.1117/12.2212011.

[23] Z. Zhong et al., "Design and fabrication of high power InGaN blue laser diode over 8 W," *Opt. Laser Technol.*, vol. 139, Jul. 2021, Art. no. 106985, doi: 10.1016/j.optlastec.2021.106985.

[24] F. Liang et al., "GaN-based blue laser diode with 6.0 W of output power under continuous-wave operation at room temperature," *J. Semicond.*, vol. 42, no. 11, Nov. 2021, Art. no. 112801, doi: 10.1088/1674-4926/42/11/112801.

[25] Crosslight Software, Inc., 2012. [Online]. Available: www.crosslight.com

[26] J. T. Yang et al., "Influence of emitter width on the performance of 975-nm (In, Ga)(As, P)/(Al, Ga) as high-power laser diodes," *Curr. Opt. Photon.*, vol. 3, no. 5, pp. 445–450, Oct. 2019, doi: 10.3807/COPP.2019.3.5.445.

[27] J. T. Yang, J. G. Kwak, A. S. Choi, T. K. Kim, and W. Y. Choi, "Lateral far-field characteristics of narrow-width 850 nm high power GaAs/AlGaAs laser diodes," *Curr. Opt. Photon.*, vol. 6, no. 2, pp. 191–195, Apr. 2022, doi: 10.1364/COPP.6.000191.

[28] J. T. Yang, Y. Kim, J. B. Lee, D. S. Bang, T. K. Kim, and W. Y. Choi, "Dependence of high-power laser diode performance on emitter width," *Proc. SPIE*, vol. 10900, 2019, Art. no. 109000N, doi: 10.1117/12.2507712.

[29] Y. Kim, Y. Sung, J. T. Yang, and W. Y. Choi, "Numerical analysis of high-power broad-area laser diode with improved heat sinking structure using epitaxial liftoff technique," *Proc. SPIE*, vol. 10514, pp. 59–64, 2018, doi: 10.1117/12.2288639.

[30] S. Nozaki et al., "High-power and high-temperature operation of an InGaN laser over 3 W at 85°C using a novel double-heat-flow packaging technology," *Jpn. J. Appl. Phys.*, vol. 55, no. 4S, Apr. 2016, Art. no. 04eh05, doi: 10.7567/jjap.55.04eh05.

[31] D. Y. Li et al., "Thermal lensing effect in ridge structure InGaN multiple quantum well laser diodes," *J. Appl. Phys.*, vol. 100, no. 4, Aug. 2006, Art. no. 046101, doi: 10.1063/1.2260658.

[32] J. Piprek, "Analysis of efficiency limitations in high-power InGaN/GaN laser diodes," *Opt. Quantum Electron.*, vol. 48, no. 10, Sep. 2016, Art. no. 471, doi: 10.1007/s11082-016-0727-3.

[33] J. Piprek, "How to decide between competing efficiency droop models for GaN-based light-emitting diodes," *Appl. Phys. Lett.*, vol. 107, no. 3, Jul. 2015, Art. no. 031101, doi: 10.1063/1.4927202.

[34] J. Piprek, "Self-consistent far-field blooming analysis for high-power Fabry-Perot laser diodes," *Proc. SPIE*, vol. 8619, pp. 227–234, 2013, doi: 10.1117/12.2004665.